

# Construction of DNA-based logic gates on nanostructured microelectrodes

Tao Wei<sup>1,2</sup> · Min Li<sup>2</sup> · Yue-Yue Zhang<sup>2</sup> · Ali Aldalbahi<sup>3</sup> · Li-Hua Wang<sup>2</sup> · Xiao-Lei Zuo<sup>2</sup> · Yun Zhao<sup>1</sup>

Received: 14 October 2016/Revised: 3 December 2016/Accepted: 19 December 2016/Published online: 2 February 2017  
© Shanghai Institute of Applied Physics, Chinese Academy of Sciences, Chinese Nuclear Society, Science Press China and Springer Science+Business Media Singapore 2017

**Abstract** Electrochemical logical operations utilizing biological molecules (protein or DNA), which can be used in disease diagnostics and bio-computing, have attracted great research interest. However, the existing logic operations, being realized on macroscopic electrode, are not suitable for implantable logic devices. Here, we demonstrate DNA-based logic gates with electrochemical signal as output combined with gold flower microelectrodes. The designed logic gates are of fast response, enzyme-free, and micrometer scale. They perform well in either pure solution or complex matrices, such as fetal bovine serum, suggesting great potential for in vivo applications.

**Keywords** Logic gates · Microelectrode · Bio-computing · Electrochemical · Nanostructured electrode

## 1 Introduction

A logic gate is a physical device implementing a Boolean function. It performs a logical operation on one or more logical inputs and produces a single logical output. Enzymes and nucleic acids are promising for constructing molecular logic gates for computational purposes [1–11], and DNA is advantageous in its high stability, suitable for bio-imaging, and precise programmability [12–17], and hence it is an excellent candidate for building logic operating systems.

Since Adleman's invention of bio-computations in 1994 using just DNA molecules [18], a diverse range of DNA logic devices have been designed [19–24]. Willner and co-workers developed fluorescent logic gates, such as 'AND,' 'OR,' and 'SET-RESET,' constructed with ions as inputs and the fluorescence intensity of a G-quadruplex as outputs [25]. Wang and co-workers constructed an optical-output 'INHIBIT' logic gate utilizing structural switched DNA probe with the addition of targets ( $K^+$  or  $Pb^{2+}$ ) [26, 27]. Kevin and co-workers reported a reagentless, molecular logic gates with electrochemical signal outputs by using electrochemical E-DNA sensor architectures on a millimeter-sized electrode [28].

So far, most of DNA-based logic gates have been constructed in bulk solution or on a macroscopic electrode at millimeter level, which hinders their in vivo applications. An electrode in micrometer or even nanometer diameter can be readily matched to the dimensions of cells and suitable for implantation in vivo [29, 30]. At SINAP, we

---

This work was supported by the National Natural Science Foundation of China (Nos. 31470960 and 21422508).

---

Authors Tao Wei and Min Li contributed equally to this work.

---

✉ Li-Hua Wang  
wanglihua@sinap.ac.cn

✉ Xiao-Lei Zuo  
zuoxiaolei@sinap.ac.cn

✉ Yun Zhao  
zhaoyun@scu.edu.cn

<sup>1</sup> Key Laboratory of Bio-Resources and Eco-Environment, Ministry of Education, College of Life Sciences, Sichuan University, Chengdu 610064, China

<sup>2</sup> Division of Physical Biology and Bioimaging Center, Shanghai Synchrotron Radiation Facility, CAS Key Laboratory of Interfacial Physics and Technology, Shanghai Institute of Applied Physics, Chinese Academy of Sciences, Shanghai 201800, China

<sup>3</sup> Chemistry Department, King Saud University, Riyadh 11451, Saudi Arabia

studied the application of gold nanoparticles in radiotherapy and synthesized gold nanostructures in different shapes [31–33]. Besides, we developed the protocol to prepare gold flower microelectrode. By immobilizing with biological probes, the gold flower microelectrode can be successfully used for small molecule (such as cocaine) detection, with fast response and high specificity [34].

In this work, we used gold flower microelectrode and developed DNA XOR logic gates, which were based on two electrochemical biosensors for ATP and DNA detections, respectively. The targets (ATP and DNA) and the denaturant urea were used as inputs, and changes in faradic current observed via square-wave voltammetry (SWV) caused by the presence or absence of targets were used as outputs (Scheme 1).

## 2 Experimental section

### 2.1 Materials

Carbon fiber ( $\Phi 7 \mu\text{m}$ ) was obtained from Toray Inc. (Japan). For microelectrode fabrication, glass capillaries (1.1 mm outer diameter, 0.9 mm inner diameter) and copper wire ( $\Phi 0.5 \text{ mm}$ ) were from Sinopharm Chemical Reagent Co. Ltd (Shanghai, China). Graphite conductive adhesive was from Ted Pella (USA), and epoxy resin was from Zhongjingkeyi Technology Co. Ltd (Nanjing, China). DNA oligonucleotides modified with a six-carbon thiol (HSC6) and the redox-active methylene blue (MB) were synthesized and purified by Sangon Biotechnology Inc. (Shanghai, China), and their sequences were as follows:

ATP sensor: 5'-HS-C6-ACCTGGGGGAGTATTGCG GAGGAAGGTTT-MB-3'.

cDNA sensor: 5'-HS-C6-GACACTGGATCGGCGTTT TATTGTGTC-MB-3'.

cDNA target: 5'AATAAAACGCCGATCCA3'.

6-Mercaptohexanol (MCH) and tris (2-carboxyethyl) phosphine hydrochloride (TCEP) were purchased from Sigma. Fetal bovine serum (FBS), qualified grade, was used as received from Life Technologies (Gibco). All other chemicals were of analytical grade, and all chemicals were used without further purification. All solutions were prepared using Milli-Q water ( $18.2 \text{ M}\Omega\text{-cm}^{-1}$ ) from a Millipore system. The buffers used were as follows: Gold electrodeposition solution included 20 mM gold chloride and 0.5 M hydrochloric acid. Tris buffer contained 20 mM Tris, 50 mM  $\text{MgCl}_2$ , pH 8.0 (TM buffer). The electrodes were rinsed in 0.1 M PBS (PBS buffer). In total, 10 mM phosphate buffer (PB) contained 20 mM  $\text{MgCl}_2$ , 1 M NaCl, pH 7.4 (PB buffer). Electrochemical detection for methylene blue (MB) was performed in 10 mM HEPES, 500 mM NaCl, pH 7.0 (HEPES buffer).

### 2.2 Electrodes preparation

Gold flower microelectrode fabrication was carried out using well-established methods [35–37]. Briefly, the glass capillary was pulled with a single-line heating and pulling program (Heat: 290; Fil: 4; Vel: 60; Del: 200; Pul: 15) using a P-2000 micropipette puller, leading to the production of two symmetric micropipette tips. Then, a single carbon fiber was attached to one end of a copper wire with graphite conductive adhesive and was carefully inserted

**Scheme 1** Design principle of electrochemical logic gates. In our design, the microelectrode with flower-like nanostructure was used to immobilize bio-probes. Here, a stem-loop structured DNA probe and an aptamer of ATP, both modified with methylene blue (MB), were employed. When the target DNA (cDNA) was introduced, the electron transfer (eT) of MB was blocked due to the conformational change of DNA structure; while when ATP was introduced, the eT was facilitated due to the conformational structure change of aptamer. (Color figure online)

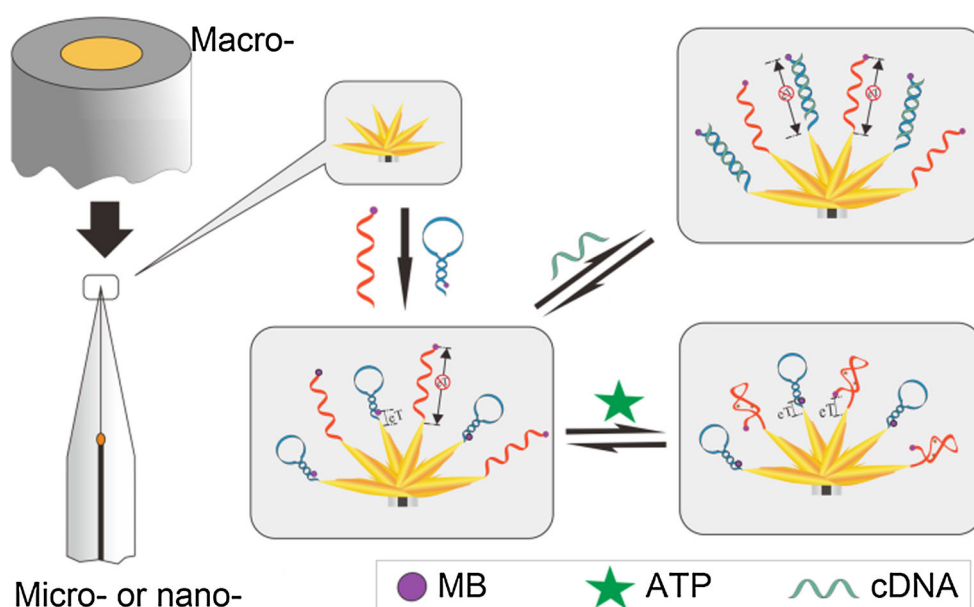


**Fig. 1** Kinetics for the ATP (a) and DNA (b) sensors in the presence of 500 nM of cDNA targets and 1 mM of ATP, respectively

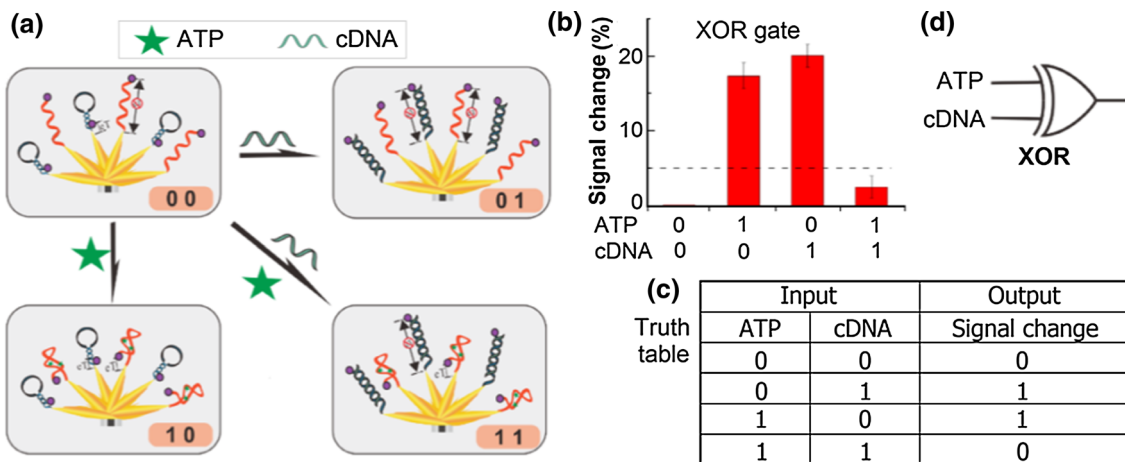
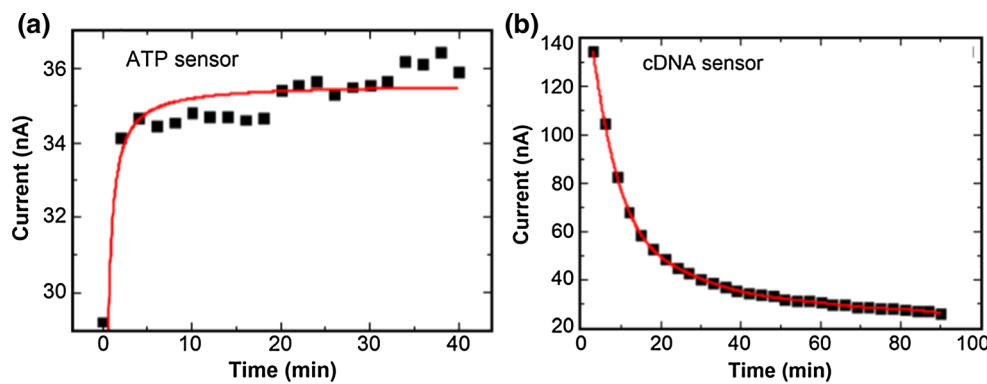


**Fig. 2** a A schematic presentation of an XOR gate. To fabricate this two-input logic device, two electrochemical DNA probes described previously, i.e., the E-DNA sensor [38–40], composed of a stem-loop oligonucleotide and E-AB sensor [38] composed of a ATP-binding DNA aptamer, attached together to a single gold flower microelectrode via an alkane thiol and modified with a redox reporter. When interrogated via square-wave voltammetry (SWV), the probes

responded to their respective targets (a complementary DNA and ATP, respectively) via decreasing and increasing faradic current, respectively. b The probes of the logic device for which four input combinations lead to different electrochemical output currents via SWV. c The truth table for this two-input logic gate. d The symbol of this logic gate

into the capillary with carbon fiber exposed to the fine open end of the capillary. The other end of the copper wire was sealed with epoxy resin. Burned and etched by flame of alcohol lamp carefully, the fine open end of the capillary was sealed with 1-mm-long carbon fiber protruding. In this way, the carbon fiber microelectrode (CFME) was acquired. Then, the gold nanoparticles (AuNPs) were electrochemically deposited on the pretreated CFME electrode in a solution of 20 mM gold chloride and 0.5 M HCl by applying a potential of 0 V versus Ag/AgCl for 200 s. Finally, rinse the gold flower microelectrodes with ultrapure water.

### 2.3 Fabrication and characterization of E-DNA sensor

The cleaned gold electrodes were soaked in TM buffer containing 1 μM DNA probes and 3 mM TCEP and allowed to immobilize overnight at room temperature. The

modified electrodes were then exposed to a 2 mM MCH solution (in PB buffer) at room temperature for 1 h to replace nonspecific interactions and form a self-assembled monolayer (SAM) that resisted nonspecific adsorption of target DNA. The electrode was rinsed with PBS buffer, and the electrochemical signals were detected using the traditional electrochemical configuration of three-electrode system. An Ag/AgCl (3 M KCl) was used as a reference electrode, and a platinum wire was used as counter electrode. Electrochemical workstation CHI 660B was used for electrochemical signal collection. The electrodes were incubated for 30 min with appropriate concentration of target in HEPES buffer or 20% fetal calf serum mixed with HEPES buffer. Considering its high sensitivity, square-wave voltammetry (SWV) was employed for the determination of ATP and cDNA. Relative signal changes in square-wave voltammetry peak current were calculated by subtracting the background current (SWV peak current in the blank buffer).

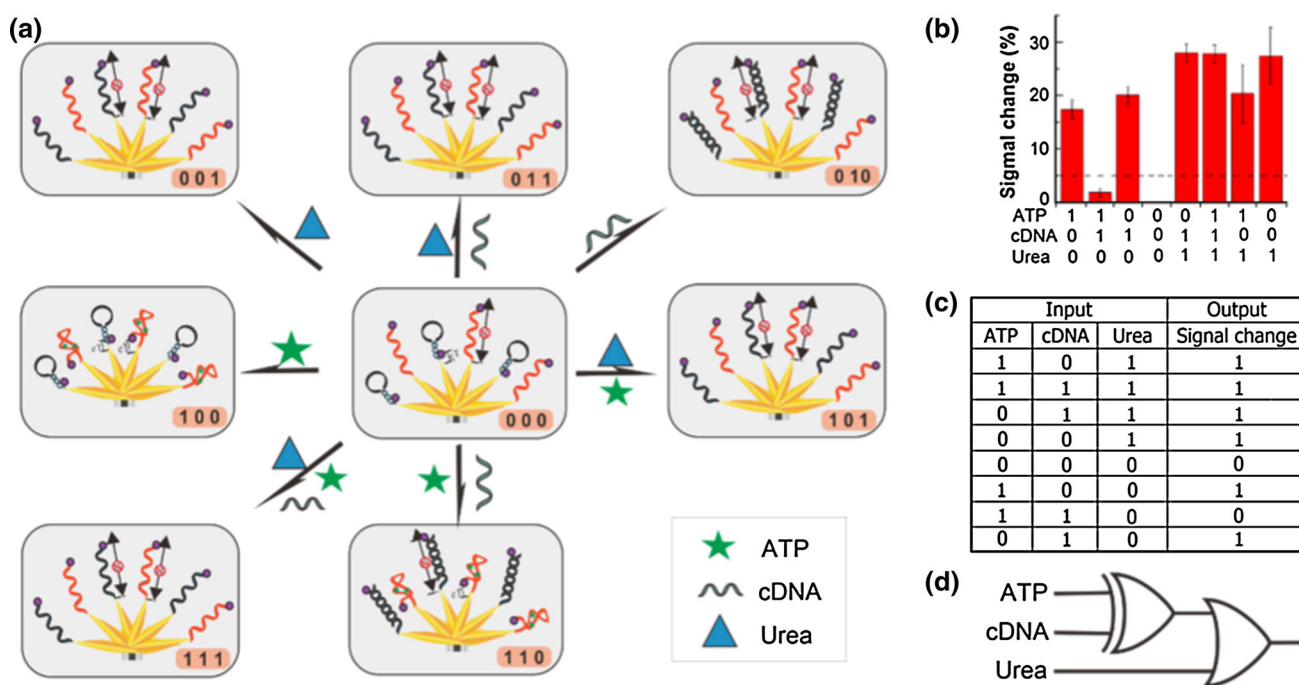
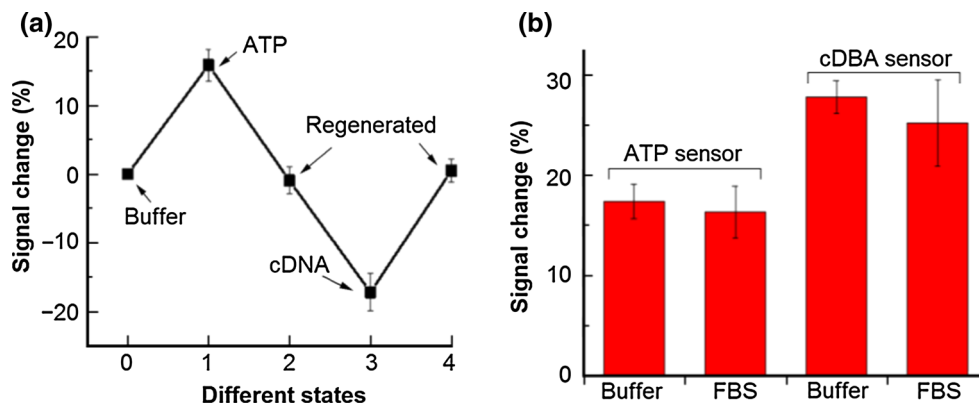


**Fig. 3** Adding denaturant urea into this two-input gate as the third input to produce a three-input logic gate. It could unfold DNA probe inducing decrease in faradic current upon SWV interrogation. **a** A schematic representation of this three-input logic gate and the

activation of the gate using varying concentrations of ATP, DNA, and urea as inputs **b** The eight input combinations induced different changes of electrochemical currents. **c** Truth table for the three-input logic gate. **d** The symbol of this logic gate

**Fig. 4** **a** Rinsing with  $1\times$ PBS, signal regeneration of this dual-analyte sensor could recover more than 90%. **b** The dual-analyte device showed similar signal change both in buffer solution and in complex samples, such as 20% FBS (diluted with HEPES buffer)



### 3 Results and discussion

We investigated the target-binding kinetics of the two electrochemical biosensors, respectively. The target-binding processes were monitored by continuously recording the SWV current peak at  $-0.25$  V (Fig. 1). The SWV current of ATP biosensor increased upon the ATP binding since the redox moiety (MB) approached the electrode surface to facilitate the electron transfer. As shown in Fig. 1, the ATP sensor demonstrated fast kinetics with a saturated time of  $\sim 5$  min. The SWV current of DNA biosensor decreased upon the DNA hybridization since the redox moiety (MB) was forced to separate from the electrode surface to block the electron transfer. Although the

DNA sensor demonstrated relatively slower target-binding kinetics than that of ATP sensor, we could still obtain the saturated signal within 30 min.

A two-analyte XOR logic device was then designed by immobilizing the two bioprobes on a single gold flower microelectrode, which compressed two input states into one output state, and the concentration of ATP and cDNA was defined as inputs, and the signal change of the faradic current resulted from methylene blue (MB) was defined as outputs. For input, we defined the presence of  $1000\ \mu\text{M}$  ATP and  $200\ \text{nM}$  cDNA as the '1' states, and lower (to 0 M) concentrations as the '0' states. As outputs, we defined signal changes of greater than 5% and less than 5% as the '1' and '0' states, respectively. Thus, we could

control the inputs (the concentration of ATP and DNA) to obtain a logic signal output and produce the truth table of our designed logic gate. The logic gate is shown schematically in Fig. 2. From the truth table, if one, and only one, of the inputs to the gate is at '1' state, the output is '1', while if both inputs are '0' states or both are '1' states, the logic gate produced an output '0.' Thus, this label-free, dual-analyte device serves as a XOR logic gate. The logic device can be designed to monitor the ratio of two inputs. For example, when two inputs (ATP and cDNA) are controlled in optimal concentration ratio of 1000  $\mu$ M ATP: 200 nM cDNA, the logic gate output is '0,' indicating that the system works well and the ratio of the two chemicals is under control. When the ratio of the two inputs shifts to a concentration ration of 0  $\mu$ M ATP: 200 nM cDNA, the output changes to '1,' indicating a state out of control that should be adjusted.

Based on the two-analyte logic device, we have also designed a three-input logic gate by using urea to this system as the third input. Urea can denature the structure of DNA probes and change the ability to transfer electrons. For input, we also defined the presence of 1 M urea as the "1" state, and lower (to 0 M) concentrations as the "0" state. As before, we defined signal changes greater than 5% and less than 5% as "1" and "0" states, respectively. As a result, a three-input logic operation was constructed by controlling the concentrations of ATP, DNA, and urea. The truth table and schematic representation of this logic gate were presented in Fig. 3.

Regeneration and stability of the logic gate were studied. The signal changed at the presence of the targets (ATP or DNA). Interestingly, through a simple rinsing by  $1 \times$  PBS, the signal could be recovered for more than 90%. Furthermore, the logic gate performed well in relatively complex sample matrices (20% FBS) and (Fig. 4). The logic device showed similar signal change both in buffer solution and in diluted FBS. Thus, the designed logic gates showed potential for the continuous monitoring in complex system.

## 4 Conclusion

In conclusion, we have constructed dual-analyte, DNA-based logic devices that functioned as an electrochemical XOR logic gate on the gold flower microelectrode. The combination of this logic gates and the gold flower microelectrode showed the advantages of electrochemical logic gate in signal readout. Most of the logic operations designed previously were realized through fluorescence output and in solution phase [2, 7, 12, 20–22, 43, 44], which may limit the connection between biological devices and electronics. Our design also reflected the application

potential of ultramicroelectrode in applications of implantable device. Most of the electrochemical logic operations that designed previously were realized on microscopic electrode [28, 42]. For some biological applications such as applications in living cells and in situ monitoring small molecules released by living cells, the scale of the electrode should be decreased to micrometers and even nanometers to fit the scale of living cells. The use of macroscopic electrode would not accomplish such tasks or result in damaging of living cells [41, 45–49].

**Acknowledgements** Ali Aldabahi acknowledges the support by the Deanship of Scientific Research, College of Science Research Center at King Saud University.

## References

1. H. Yan, Nucleic acid nanotechnology. *Science* **306**, 2048–2049 (2004). doi:10.1126/science.1106754
2. M.N. Stojanovic, D. Stefanovic, A deoxyribozyme-based molecular automaton. *Nat. Biotechnol.* **21**, 1069–1074 (2003). doi:10.1038/nbt862
3. N.C. Seeman, From genes to machines: DNA nanomechanical devices. *Trends Biochem. Sci.* **30**, 119–125 (2005). doi:10.1016/j.tibs.2005.01.007
4. A.P. de Silva, S. Uchiyama, Molecular logic and computing. *Nat. Nanotechnol.* **2**, 399–410 (2007). doi:10.1038/nnano.2007.188
5. A. Condon, Designed DNA molecules: principles and applications of molecular nanotechnology. *Nat. Rev. Genet.* **7**, 565–575 (2006). doi:10.1038/nrg1892
6. P.R. Solanki, A. Kaushik, V.V. Agrawal et al., Nanostructured metal oxide-based biosensors. *NPG Asia Mater.* **3**, 17–24 (2011). doi:10.1038/asiamat.2010.137
7. M. Motornov, J. Zhou, M. Pita et al., "Chemical transformers" from nanoparticle ensembles operated with logic. *Nano Lett.* **8**, 2993–2997 (2008). doi:10.1021/nl802059m
8. J. Li, Self-assembled supramolecular hydrogels based on polymer-cyclodextrin inclusion complexes for drug delivery. *NPG Asia Mater.* **2**, 112–118 (2010). doi:10.1038/asiamat.2010.84
9. J.R. Heath, M.A. Ratner, Molecular electronics. *Phys. Today* **56**, 43–49 (2003). doi:10.1063/1.1583533
10. J.M. Tour, Molecular electronics, synthesis and testing of components. *Acc. Chem. Res.* **33**, 791–804 (2000). doi:10.1021/ar0000612
11. B. Ding, N.C. Seeman, Operation of a DNA robot arm inserted into a 2D DNA crystalline substrate. *Science* **314**, 1583–1585 (2006). doi:10.1126/science.1131372
12. W. Li, F. Zhang, H. Yan et al., DNA based arithmetic function: a half adder based on DNA strand displacement. *Nanoscale* **8**, 3775–3784 (2016). doi:10.1039/c5nr08497k
13. X.H. Mao, J.C. Du, Q. Huang et al., Application of super-resolution microscopy in biology. *Nucl. Tech.* **36**, 060502–1–060502-8 (2013). doi:10.11889/j.0253-3219.2013.hjs.36.060502. (in Chinese)
14. Y. Tian, Y. Wang, Y. Xu et al., A highly sensitive chemiluminescence sensor for detecting mercury (II) ions: a combination of Exonuclease III-aided signal amplification and graphene oxide-assisted background reduction. *Sci. China Chem.* **58**, 514–518 (2015). doi:10.1007/s11426-014-5258-9
15. P.J. Wang, Y. Wan, A. Ali et al., Aptamer-wrapped gold nanoparticles for the colorimetric detection of omethoate. *Sci.*

- China Chem. **59**, 237–242 (2016). doi:10.1007/s11426-015-5488-5
16. J. Chao, C.H. Fan, A photoelectrochemical sensing strategy for biomolecular detection. *Sci. China Chem.* **58**, 834 (2015). doi:10.1007/s11426-015-5402-1
17. S.G. Hou, L. Liang, S.H. Deng et al., Nanoprobes for super-resolution fluorescence imaging at the nanoscale. *Sci. China Chem.* **57**, 100–106 (2014). doi:10.1007/s11426-013-5014-6
18. L.M. Adleman, Molecular computation of solutions To combinatorial problems. *Science* **266**, 1021–1024 (1994). doi:10.1126/science.7973651
19. O.A. Bozdemir, R. Guliyev, O. Buyukcakir et al., Selective manipulation of ICT and PET processes in styryl-bodipy derivatives: applications in molecular logic and fluorescence sensing of metal ions. *J. Am. Chem. Soc.* **132**, 8029–8036 (2010). doi:10.1021/ja1008163
20. J. Macdonald, Y. Li, M. Sutovic et al., Medium scale integration of molecular logic gates in an automaton. *Nano Lett.* **6**, 2598–2603 (2006). doi:10.1021/nl0620684
21. F. Pu, Z. Liu, X.J. Yang et al., DNA-based logic gates operating as a biomolecular security device. *Chem. Commun.* **47**, 6024–6026 (2011). doi:10.1039/c1cc11280e
22. T. Li, L.B. Zhang, J. Ai et al., Ion-Tuned DNA/Ag fluorescent nanoclusters as versatile logic device. *ACS Nano* **5**, 6334–6338 (2011). doi:10.1021/nn201407h
23. M. Ogiwara, A. Ray, Molecular computation: DNA computing on a chip. *Nature* **403**, 143–144 (2000). doi:10.1038/35003071
24. Y. Benenson, B. Gil, U. Ben-Dor et al., An autonomous molecular computer for logical control of gene expression. *Nature* **429**, 423–429 (2004). doi:10.1038/nature02551
25. M. Moshe, J. Elbaz, I. Willner, Sensing of  $\text{UO}_2^{2+}$  and design of logic gates by the application of supramolecular constructs of ion-dependent DNazymes. *Nano Lett.* **9**, 1196–1200 (2009). doi:10.1021/nl803887y
26. X. Feng, X. Duan, L. Liu et al., Fluorescence logic-signal-based multiplex detection of nucleases with the assembly of a cationic conjugated polymer and branched DNA. *Angew. Chem.* **48**, 5316–5321 (2009). doi:10.1002/anie.200901555
27. T. Li, E.K. Wang, S.J. Dong, Potassium-Lead-Switched G-Quadruplexes: a new class of DNA logic gates. *J. Am. Chem. Soc.* **131**, 15082–15083 (2009). doi:10.1021/ja9051075
28. F. Xia, X.L. Zuo, R.Q. Yang et al., Label-Free, dual-analyte electrochemical biosensors: a new class of molecular-Electronic logic gates. *J. Am. Chem. Soc.* **132**, 8557–8559 (2010). doi:10.1021/ja101379k
29. M.A. Makos, K.A. Han, M.L. Heien et al., Using in vivo electrochemistry to study the physiological effects of cocaine and other stimulants on the drosophila melanogaster dopamine transporter. *Acs Chem. Neurosci.* **1**, 74–83 (2010). doi:10.1021/cn900017w
30. Y. Takahashi, A.I. Shevchuk, P. Novak et al., Multifunctional nanoprobes for nanoscale chemical imaging and localized chemical delivery at surfaces and interfaces. *Angew. Chem. Int. Edit.* **50**, 9638–9642 (2011). doi:10.1002/anie.201102796
31. M.M. Liu, K. Wang, N. Chen et al., Radiotherapy enhancement with gold nanoparticles. *Nucl. Tech.* **38**, 51–56 (2015). doi:10.11889/j.0253-3219.2015.hjs.38.090501. (in Chinese)
32. G.S. Wei, F.W. Xiang, T. Tian et al., Application of gold nanoparticles in tumor detection and radiation therapy. *Radiat. Res. Radiat. Process.* **34**, 040103–2–040103-6 (2016). doi:10.11889/j.1000-3436.2016.rj.34.040103. (in Chinese)
33. J.L. Shen, Y. Xu, K. Li et al., Synthesis of dumbbell-like Au nanostructure and its light-absorbance study. *Nucl. Tech.* **36**, 060501–1–060501-6 (2013). doi:10.11889/j.0253-3219.2013.hjs.36.060501. (in Chinese)
34. D. Zhu, M. Li, L.H. Wang et al., A micro E-DNA sensor for selective detection of dopamine in presence of ascorbic acid. *Nucl. Sci. Tech.* **26**, 115–119 (2015). doi:10.13538/j.1001-8042/nst.26.060504
35. Y.P. Luo, L.M. Zhang, W. Liu et al., A single biosensor for evaluating the levels of copper ion and L-Cysteine in a live rat brain with Alzheimer's disease. *Angew. Chem. Int. Edit.* **54**, 14053–14056 (2015). doi:10.1002/anie.201508635
36. W.H. Huang, D.W. Pang, H. Tong et al., A method for the fabrication of low-noise carbon fiber nanoelectrodes. *Anal. Chem.* **73**, 1048–1052 (2001). doi:10.1021/ac0008183
37. D. Zhu, X.L. Zuo, C.H. Fan, Fabrication of nanometer-sized gold flower microelectrodes electrochemical biosensing applications. *Sci. China Chem.* **45**, 1214–1219 (2015). doi:10.1360/N032015-00039. (in Chinese)
38. X.L. Zuo, S.P. Song, J. Zhang et al., A target-responsive electrochemical aptamer switch (TREAS) for reagentless detection of nanomolar ATP. *J. Am. Chem. Soc.* **129**, 1042–1043 (2007). doi:10.1021/ja067024b
39. J. Zhang, S.P. Song, L.H. Wang et al., A gold nanoparticle-based chronocoulometric DNA sensor for amplified detection of DNA. *Nat. Protoc.* **2**, 2888–2895 (2007). doi:10.1038/nprot.2007.419
40. C.H. Fan, K.W. Plaxco, A.J. Heeger, Electrochemical interrogation of conformational changes as a reagentless method for the sequence-specific detection of DNA. *Proc. Natl. Acad. Sci. U.S.A.* **100**, 9134–9137 (2003). doi:10.1073/pnas.1633515100
41. F.B. Meng, Y.M. Hervault, Q. Shao et al., Orthogonally modulated molecular transport junctions for resettable electronic logic gates. *Nat. Commun.* (2014). doi:10.1038/Ncomms4023
42. D.F. Wang, Y.M. Fu, J. Yan et al., Molecular logic gates on DNA origami nanostructures for MicroRNA diagnostics. *Anal. Chem.* **86**, 1932–1936 (2014). doi:10.1021/ac403661z
43. E.M. Cornett, E.A. Campbell, G. Gulenay et al., Molecular logic gates for DNA analysis: detection of rifampin resistance in *M. tuberculosis* DNA. *Angew. Chem. Int. Edit.* **51**, 9075–9077 (2012). doi:10.1002/anie.201203708
44. S. Erbas-Cakmak, E.U. Akkaya, Cascading of molecular logic gates for advanced functions: a self-reporting activatable photosensitizer. *Angew. Chem. Int. Edit.* **52**, 11364–11368 (2013). doi:10.1002/anie.201306177
45. R. Pan, M.C. Xu, D.C. Jiang et al., Nanokit for single-cell electrochemical analyses. *Proc. Natl. Acad. Sci. U.S.A.* **113**, 11436–11440 (2016). doi:10.1073/pnas.1609618113
46. S. Umehara, M. Karhanek, R.W. Davis et al., Label-free biosensing with functionalized nanopipette probes. *Proc. Natl. Acad. Sci. U.S.A.* **106**, 4611–4616 (2009). doi:10.1073/pnas.0900306106
47. J.E. Dick, A.T. Hilterbrand, A. Boika et al., Electrochemical detection of a single cytomegalovirus at an ultramicroelectrode and its antibody anchoring. *Proc. Natl. Acad. Sci. U.S.A.* **112**, 5303–5308 (2015). doi:10.1073/pnas.1504294112
48. F.O. Laforge, J. Carpino, S.A. Rotenberg et al., Electrochemical attosyringe. *Proc. Natl. Acad. Sci. U.S.A.* **104**, 11895–11900 (2007). doi:10.1073/pnas.0705102104
49. B.P. Helmke, A.R. Minerick, Designing a nano-interface in a microfluidic chip to probe living cells: challenges and perspectives. *Proc. Natl. Acad. Sci. U.S.A.* **103**, 6419–6424 (2006). doi:10.1073/pnas.0507304103